Published in final edited form as:
Cell Rep. 2014 March 27; 6(6): 1096–1109. doi:10.1016/j.celrep.2014.02.010.

Calsyntenins Function as Synaptogenic Adhesion Molecules in Concert with Neurexins

Ji Won Um[1], **Gopal Pramanik**[2,3], **Ji Seung Ko**[1], **Min-Young Song**[4], **Dongmin Lee**[5], **Hyun Kim**[5], **Kang-Sik Park**[4], **Thomas C. Südhof**[6], **Katsuhiko Tabuchi**[2,3,7], and **Jaewon Ko**[1,#]

[1]Department of Biochemistry, College of Life Science and Biotechnology, Yonsei University, Seoul 120-749, Korea

[2]Dept. of Molecular and Cellular Physiology, Shinshu University School of Medicine, Matsumoto 390-8621, Japan

[3]Division of Cerebral Structure, Dept. of Cerebral Research, National Institute for Physiological Sciences, Okazaki 444-8787, Japan

[4]Department of Physiology and Neuroscience, Kyung Hee University School of Medicine, Seoul 130-701, Korea

[5]Department of Anatomy and Neuroscience, Korea 21 Biomedical Science, College of Medicine, Korea University, 126-1, 5-ka, Anam-dong, Seongbuk-gu, Seoul 136-705, Korea

[6]Department of Molecular and Cellular Physiology and Howard Hughes Medical Institute, Stanford University School of Medicine, Stanford, CA 94305, USA

[7]PRESTO, Japan Science and Technology Agency (JST), Kawaguchi 332-0012, Japan

SUMMARY

Multiple synaptic adhesion molecules govern synapse formation. Here, we propose calsyntenin-3/alcadein-β as a synapse organizer that specifically induces presynaptic differentiation in heterologous synapse-formation assays. Calsyntenin-3 (CST-3) was highly expressed during various postnatal periods of mouse brain development. The simultaneous knockdown of all three CSTs, but not CST-3 alone, decreased inhibitory, but not excitatory, synapse densities in cultured hippocampal neurons. Moreover, the knockdown of CSTs specifically reduced inhibitory synaptic transmission *in vitro* and *in vivo*. Remarkably, the loss of CSTs induced a concomitant decrease in neuron soma size in a non-cell-autonomous manner. Furthermore, α-neurexins (α-Nrxs) were affinity-purified as components of a CST-3 complex involved in CST-3-mediated presynaptic differentiation. However, CST-3 did not directly bind to Nrxs. Viewed together, these data suggest

[#]Correspondence should be addressed to Jaewon Ko (jaewonko@yonsei.ac.kr).

SUPPLEMENTAL INFORMATION

Supplemental Information includes 7 Supplemental Figures, 2 Supplemental Tables, and Extended Experimental Procedures and can be found with this article online at http://cellreports.cell.com/

that the three CSTs redundantly regulate inhibitory synapse formation, inhibitory synapse function, and neuron development in concert with Nrxs.

Keywords

calsyntenin-3; neurexin; synapse function; synaptic adhesion

INTRODUCTION

Synaptic cell adhesion molecules (CAMs) are major synapse organizers that initiate the cell type-specific formation of nascent synaptic contacts and recruit the pre- and postsynaptic protein complexes required for proper synaptic signaling (Missler et al., 2012). The list of synaptic CAMs has rapidly grown, largely reflecting the development of the heterologous synapse formation assay (Biederer and Scheiffele, 2007). Neuroligins (NLs), SynCAMs, Netrin-G ligands (NGLs), SALM3 and SALM5, Leucine-rich repeat transmembrane proteins (LRRTMs), and Slit- and Trk-like (Slitrks) proteins are among the synaptogenic CAMs with established synaptic functions (Missler et al., 2012; Sudhof, 2008; Um and Ko, 2013). However, considering the number of neuronal synapses and neural circuits in the brain, it is reasonable to propose that additional synaptogenic CAMs remain undefined.

Calsyntenins (CSTs), called alcadeins, are members of the cadherin superfamily (Araki et al., 2003; Vogt et al., 2001). Originally identified from spinal cord neurons (Vogt et al., 2001), CSTs are type I transmembrane proteins with extracellular domains containing two cadherin repeats and an LNS (laminin-α, neurexin, and sex hormone-binding globulin) domain. These proteins comprise three members: CST-1 (alcadein-α), CST-2 (alcadein-γ), and CST-3 (alcadein-β), and a single ortholog has also been identified in *Caenorhabditis elegans* (CASY-1 or CDH11) and *Drosophila melanogaster* (Cals) (Ikeda et al., 2008; Pettitt, 2005). CSTs are widely expressed in the central nervous system (Hintsch et al., 2002; Vogt et al., 2001). CST-1 is primarily expressed in the postsynaptic membranes of pyramidal neurons, whereas CST-2 and -3 are expressed in inhibitory neurons (Hintsch et al., 2002). Interestingly, CASY-1 is essential for chemotaxis-associated learning (Hoerndli et al., 2009; Ikeda et al., 2008), and CST-2 polymorphisms have been associated with human memory performance (Papassotiropoulos et al., 2006). In addition, CSTs dock vesicular cargo to kinesin-1, thereby determining the identity of transported cargo molecules (Araki et al., 2007; Konecna et al., 2006; Maruta et al., 2012; Vagnoni et al., 2011). More specifically, CST-1 mediates the transport of amyloid precursor protein (APP) via binding to X11/Mint and protects this protein from proteolytic processing during axonal transport (Suzuki et al., 2006; Vagnoni et al., 2012). Intriguingly, several CST peptides have been frequently identified in the cerebrospinal fluid of Alzheimer's disease (AD) patients (Ringman et al., 2012; Yin et al., 2009), and CST-3 accumulates in dystrophic neurites surrounding Amyloid-β (Aβ) plaques (Uchida et al., 2013). Moreover, CST-1 regulates Aβ production through the regulation of APP transport at axons (Vagnoni et al., 2012). These data suggest that CST-associated molecular pathways might contribute to the pathogenic mechanisms underlying AD. However, the synaptic functions of CSTs have not been investigated.

Here, we characterized the effects of CSTs on the structure and function of synapses in hippocampal and somatosensory cortical layer II/III neurons *in vivo*. CST-3 specifically induced presynaptic differentiation. The simultaneous knockdown of all three CSTs, but not a single CST isoform, decreased inhibitory synapse densities in cultured hippocampal neurons. Strikingly, CST-deficient neurons were morphologically smaller, and the neuronal phenotype was completely restored through the exogenous expression of full-length CST proteins. Furthermore, the frequency of miniature inhibitory, but not excitatory, postsynaptic currents was specifically reduced in CST-deficient cultured hippocampal and somatosensory cortical neurons. Moreover, we observed that CST-3 forms functional (but not physical) complexes with Nrxs. These data suggest that CST-3 is a synaptogenic adhesion molecule that forms functional complexes with Nrxs to regulate inhibitory synapse function.

RESULTS

Using heterologous synapse-formation assays with plasmid vectors expressing the entire extracellular region of cell-surface proteins exhibiting brain-specific expression (Table S1), we screened for novel synaptogenic molecules that induce presynaptic differentiation (Biederer and Scheiffele, 2007). The results revealed that LRRTMs, Slitrks, and TrkC act at the axons of cocultured neurons to specifically trigger presynaptic differentiation (Ko et al., 2009a; Yim et al., 2013). In addition, the expression of CST-3 also showed synaptogenic activity.

CST-3 Triggers Presynaptic Differentiation

To determine the synaptic function(s) of CST-3, we first examined whether all three CSTs trigger presynaptic differentiation in heterologous synapse-formation assays using HEK293T cells expressing each CST protein. To maximize the cell surface expression of CST proteins, we generated plasmids for the expression of full extracellular fragments of CSTs. CST-3, but not CST-1 or CST-2, strongly induced synapsin clustering (Figures 1A and 1B). In parallel experiments, CALS, the Drosophila ortholog of mammalian CSTs, did not induce synaptic clustering (**data not shown**). Similar to NL-2 (positive control), CST-3 induced the synaptic clustering of both the excitatory presynaptic marker VGLUT1 (vesicular glutamate transport 1) and the inhibitory presynaptic marker GAD67 (glutamic acid decarboxylase, 67 kDa), but not the excitatory postsynaptic marker PSD-95 (postsynaptic density, 95 kDa) (Figures 1A and 1B). These results suggest that CST-3 is a novel postsynaptogenic factor that induces presynaptic differentiation.

N-terminal Cadherin Repeats Are Essential for the Presynapse-inducing Activities of CST-3

CSTs possess two extracellular cadherin motifs (Cad repeats), a single LG/LNS domain, a transmembrane segment, and a short intracellular region comprising X11- and kinesin-binding sites (Araki et al., 2003; Vogt et al., 2001). To determine the domains responsible for CST-3 synaptogenic activity, we performed heterologous synapse-formation assays using deletion constructs of CST-3 extracellular fragments (Figure 2A). Only CST-3 mutants containing both Cad repeats exhibited full synaptogenic activity in heterologous synapse-formation assays (Figures 2B and 2C). Cadherin repeats typically mediate

extracellular Ca^{2+}-dependent homophilic adhesion; thus, we examined whether CSTs mediate homo- or heterophilic adhesion between CST family members using cell-adhesion and cell surface-labeling assays (Figure S1). We observed that CSTs showed no homo- or heterophilic adhesion activities, suggesting the existence of unidentified presynaptic ligand(s) for CSTs.

CST-3 mRNA and Protein Expression Patterns

Previous Northern blot and *in situ* hybridization analyses of CSTs revealed that these proteins are located in postsynaptic membranes and are widely expressed in multiple brain regions (Hintsch et al., 2002; Vogt et al., 2001). Intriguingly, although CST-1 is enriched in axonal growth cone vesicles in the developing brain, this protein is restricted to the postsynaptic membranes of excitatory and inhibitory synapses (Konecna et al., 2006; Vogt et al., 2001). To determine whether other CST isoforms are also expressed in the developing brain, we performed *in situ* hybridization using mouse brain sections obtained from various embryonic and postnatal developmental stages (Figure 3A). CST-1 mRNA was expressed through the entire body, and more abundantly in the central nervous system (Figure 3A), consistent with the previously reported CST-1 expression pattern (Vogt et al., 2001). In contrast, the distribution of CST-2 and CST-3 in E16-E18 mice was restricted to the central nervous system. In adult mouse brains, a strong CST-3 mRNA signal was observed in various brain areas, whereas CST-2 mRNA was locally distributed to brain regions, including the hippocampus and olfactory bulb (Figure 3A).

To confirm the results obtained in the *in situ* hybridization analysis, we generated CST polyclonal CST-1/CST-2 antibodies (pan-antibody, JK010) and a CST-3-specific antibody (JK001) (Figures 3B and 3C). The CST-3 antibody (JK001) was used to confirm the authenticity of the immunoreactive signals using CST-3-knockout mouse lysates (Figure 3D). The expression of CST-1/CST-2 proteins abruptly increased between postnatal day 7 (P7) and P14, whereas CST-3 protein was steadily expressed throughout the postnatal development of mouse brains (Figure 3E). However, these antibodies were not suitable for immunocytochemistry; thus, we were unable to determine the synaptic localization of CSTs in cultured neurons (**data not shown**). All three CST proteins were significantly expressed (although not clearly enriched) in the PSD fraction (Figure 3F), consistent with previously reported biochemical data (Vogt et al., 2001). Taken together, these results indicate that CST-3 is a PSD-localized synaptogenic adhesion molecule.

The Simultaneous Knockdown of All Three CSTs Decreases Inhibitory Synapse Density in Cultured Neurons

To determine whether CSTs are required for the maintenance of synapse structure, we generated a series of knockdown (KD) lentiviral vectors expressing short hairpin RNA (shRNA) targeting individual CSTs. Subsequently, we infected cultured mouse cortical neurons with these vectors, and assessed the endogenous target mRNA and protein levels using quantitative real-time reverse transcription-polymerase chain reaction (RT-PCR) and quantitative immunoblotting, respectively (Figures 4A and 4B). The shRNA suppressed endogenous mRNA expression ~90% for CST-1, ~80% for CST-2, and ~85% for CST-3 (Figure 4B). We next investigated whether the single KD of CST-1, CST-2, or CST-3

altered the synapse number in cultured mouse hippocampal neurons. To this end, we infected cultured neurons at DIV3 with lentiviruses expressing only EGFP (Control) or co-expressed EGFP with shRNAs against CST-1 (J73), CST-2 (J76), or CST-3 (J81). In addition, we immunostained neurons at DIV14 for synapsin and MAP2 to visualize the entire somatodendritic architecture of the infected neurons (Figure S2A). We observed that single KD of each CST did not alter synapse density, synapse size, synapse strength or soma size (Figures S2B–S2E), suggesting that either CSTs are not required for synapse maintenance or that CSTs are functionally redundant. To examine the potential functional redundancy of CSTs, we generated a triple-KD vector (CST-TKD) containing three human polymerase III promoters to drive the expression of shRNAs against all three CSTs and a ubiquitin promoter to drive expression of EGFP, facilitating the visualization of infected or transfected neurons (Figure 4A).

Using the CST-TKD vector, which successfully suppressed the mRNA levels of all three CSTs (Figure 4C), we examined whether CSTs are functionally redundant and essential for synapse maintenance in cultured hippocampal neurons (Figures 4 and S3). Strikingly, CST-TKD significantly decreased the number of inhibitory synapses, assessed using inhibitory synaptic markers (GAD67 and gephyrin) (Figures 4D, 4E and S3). CST-TKD also significantly reduced the number of excitatory presynaptic puncta (labeled by VGLUT1), but not excitatory postsynaptic puncta (labeled by Homer1) (Figures 4D, 4E and S3). These data suggest that CST-TKD preferentially alters inhibitory, but not excitatory, synapse structure in cultured hippocampal neurons. As previously reported, an LRRTM1 and LRRTM2 double-KD vector (LRRTM-DKD) did not alter the synapse density (Figures 4D and 4E; (Ko et al., 2011)). We also transfected cultured neurons at DIV8 with CST-TKD or an empty lentiviral shRNA vector (Control) and immunostained neurons at DIV14 for synapsin and EGFP (Figure S4). The introduction of the CST-TKD vector induced a modest but significant decrease in synapse number without changing synapse or soma size, or any spine parameters (number, width or length) (Figures S4A–S4G). Taken together, these results suggest that CSTs redundantly maintain synapses in cultured hippocampal neurons.

KD of CSTs Decreases the Soma Size of Cultured Hippocampal Neurons

An analysis of cultured mouse neurons infected with CST-TKD lentiviruses showed a dramatic reduction in the soma size of CST-TKD-infected neurons compared with control or LRRTM-DKD-infected neurons (Figures 4D and 4F). Moreover, electrophysiology recordings in cultured hippocampal neurons revealed that CST-TKD caused a significant decrease in membrane capacitance (C_m) and a concomitant increase in input resistance (R_m) (Figures S5A and S5B). These results imply that CSTs might stimulate the development of hippocampal neurons during the early stages of development. To examine this hypothesis, we infected hippocampal neurons with Control or CST-TKD viruses at DIV3 and measured neuron soma size during cultured neuron development every other day from DIV5 to DIV13 (Figures S6). We observed that the soma size of cultured neurons infected with control viruses abruptly increased between DIV7 and DIV9, whereas no increase in the soma size of neurons infected with CST-TKD was observed (Figures S6), suggesting that a deficiency of CST proteins arrests neuronal development, which manifests as an absence of growth in the cell body size. In contrast, the soma size of neurons transfected with CST-TKD was

unchanged (Figures S4D), indicating that the effects of CSTs in regulating neuronal soma size were non-cell-autonomous. Because the simultaneous KD of multiple proteins occasionally leads to confounding, non-specific phenotypes, we further examined whether the decreases in soma size and synapse number induced through CST-TKD could be rescued through the co-expression of shRNA-resistant CSTs (Figures 4G, 4H and 4I). We observed that superinfection with both CST-1 and CST-3 completely eliminated the deficits in both soma size and synapse density observed with CST-TKD (Figures 4G, 4H and 4I). Strikingly, the super-infection of either CST-1 or CST-3 alone did not restore the deficits in soma size, but did restore the deficits in synapse number, suggesting that all three CSTs contribute to the growth of the neuronal cell body in a concerted manner. We also noted that the lentiviral expression of CST-1, CST-2, or CST-3 alone did not affect synapse density (Figure 4H). Thus, we considered whether our lentiviral expression system yielded lower expression levels of CSTs than chemical transfection. Thus, we compared the effect of expressing CST-3 in cultured hippocampal neurons using a CST-3 lentiviral construct with CST-3 expression plasmid transfection using a Ca^{2+}-phosphate/DNA coprecipitation method (Figures S7A, S7B and S7C). The overexpression of CST-3 by chemical transfection significantly increased the synapse density, whereas lentiviral CST-3 expression did not, implying that the CST-3 expression level per se is critical for synapse maintenance (Figures S7A, S7B and S7C). Using the CST-3 WT expression vector, we found that CST-3 WT exerted synaptogenic activities in gain-of-function assays. CSTs are cleaved by α-secretases (Maruta et al., 2012), raising questions concerning the expression of these CST constructs on the surface of heterologous cells and neurons. We found that, although the majority of CSTs are secreted into the cell culture medium, 10–35% of CSTs are expressed on the surface of both HEK293T cells and cultured neurons (Figures S7D, S7E, S7F, S7G and **data not shown**), suggesting that surface-exposed CSTs remain competent.

KD of CSTs Leads to a Reduction in Inhibitory, but Not Excitatory, Synaptic Transmission *In Vitro* and *In Vivo*

To determine whether the changes in anatomical synapse numbers presented in Figure 4 reflect changes in the number of functional synapses, we examined synaptic transmission in mouse cultured hippocampal neurons infected with control or CST-TKD viruses (Figures S5C–S5H). Strikingly, measurements of miniature excitatory postsynaptic currents (mEPSCs) showed that CST-TKD did not alter excitatory synaptic transmission (Figures S5C and S5E-S5F). In contrast, CST-TKD caused a significant decrease in the frequency, but not the amplitude, of miniature inhibitory postsynaptic currents (mIPSCs) (Figures S5D and S5G–S5H). These results suggest that, although CSTs are required for the maintenance of both excitatory and inhibitory synapses, these molecules are predominantly involved in regulating inhibitory synaptic functions.

To further corroborate the *in vitro* electrophysiological results, we examined the effect of CSTs KD in somatosensory cortical layer II/III neurons *in vivo* through the *in utero* electroporation at E15 and analysis at P14–19 (Figure 5A). Similar to the results obtained with cultured neurons, CST-TKD specifically reduced the frequency of mIPSCs (Figures 5B, 5C and 5D) without altering the frequency or amplitude of mEPSCs (Figures 5E, 5F and 5G). Unexpectedly, CST-TKD increased the amplitude of mIPSCs. The explanation for this

observation is not clear, but might reflect the increased soma size of CST-deficient neurons or increased gephyrin puncta intensity (see Figures 5J and 5K; see also Figure 4; **data not shown**). We detected no changes in the paired-pulse ratio (PPR) of inhibitory IPSCs in CST-TKD neurons, indicating no effects on presynaptic functions (Figures 5H and 5I). Consistent with the cultured neuron morphology, the soma sizes of CST-TKD neurons were smaller, as demonstrated by a decrease in membrane capacitance and a trend toward increased input resistance (Figures 5J and 5K). Taken together, these results indicate that CSTs are required for inhibitory synaptic transmission *in vitro* and *in vivo*.

CST-3 Forms Functional Complexes with Nrxs to Induce Presynapse Development

CSTs contain two extracellular cadherin-repeats and an LNS domain, and CST-3 displays synaptogenic activity, inducing presynaptic differentiation in heterologous synapse-formation assays (Figures 1 and 2). To identify proteins that interact with the extracellular regions of CST-3, we used affinity chromatography, employing recombinant CST-3 fusion proteins expressed from HEK293T cells transfected with Ig-CST-3 comprising the entire extracellular sequence of CST-3 fused to the Fc-domain of human IgG to probe solubilized mouse brains (Figure 6A). Mass spectrometry analyses of Coomassie Blue-stained gels revealed multiple bands that were not observed in the negative control lane (IgC; Figure 6B). Among the identified peptides, multiple peptides were derived from cell surface proteins, such as Nrxs (Figures 6C, 6D, 6E, 6F, Table 1 and Table S2). We asked whether Nrxs are required for the synaptogenic activities of CST-3. We infected cultured neurons with lentiviruses expressing either an empty shRNA vector (Control) or a triple KD shRNA construct for Nrxs (Nrx-TKD). Subsequently, we performed heterologous synapse-formation assays using infected neurons and HEK293T cells expressing CST-3, neuroligin-1 (NL1; positive control) or Slitrk1 (negative control) (Figures 6G and 6H). Upon Nrx-TKD, we observed the absence of CST-3 induced synapsin clustering on contacting axons of co-cultured hippocampal neurons. In parallel experiments, Nrx-TKD abolished the synaptogenic activities of NL1 but not those of Slitrk1, consistent with the notion that Nrxs are presynaptic receptors for NL1 (note that PTPδ and PTPσ are presynaptic ligands for Slitrk1; see (Gokce and Sudhof, 2013; Yim et al., 2013)). Taken together, these results indicate that CST-3 forms a functional complex with Nrxs.

CST-3 Does Not Directly Interact with Nrxs

The fact that presynaptic Nrxs are functional receptors for CST-3 (Figure 6) prompted us to examine whether Nrxs directly bind to CST-3. First, we employed cell surface-labeling assays to determine whether CST-3 directly binds to both α- and β-Nrxs (Figures 7A and 7B). We examined the binding of recombinant Ig-fusion proteins of Nrx-1α and −1β lacking an insert in splice site #4 (Ig-Nrx1α^{SS4-} and Ig-Nrx1β^{SS4-}, respectively) to HEK293T cells expressing HA-tagged CSTs. Surprisingly, we observed no binding of the Ig-Nrx1 fusion proteins with HA-CSTs in cell surface-labeling assays (Figure 7A). Consistent with this observation, we found that the Ig-CST-3 fusion protein did not bind FLAG-tagged Nrxs in cell surface-labeling assays (Figure 7B). There are three alternative splicing sites unique to α-Nrxs (Ullrich et al., 1995); thus we hypothesized that the presence of inserts at any or all of these sites (SS#1, SS#2, and SS#3) might modulate the binding between CST-3 and α-Nrxs in a combinatorial manner. To examine this hypothesis, we generated a series of

Nrx-1α constructs containing a subset of domains with selected splice variants (see Figure 7C for schematic diagrams of HA-Nrx-1α constructs) and analyzed the binding of these proteins to recombinant CST-3 using cell surface-labeling assays (Figure 7D). Strikingly, any Nrx1α variants showed no robust binding to HA-CST-3, indicating that Nrx-1α is not a direct ligand for CST-3. Moreover, neither Nrx-2α nor Nrx-3α interacted with CST-3 in cell surface-labeling assays (Figure 7D). Consistently, we found that CST-3 Cad did not bind to Nrx1α, suggesting that CST-3 exerts synaptogenic activity through a mechanism independent of direct binding to Nrxs (Figure 7A). Furthermore, pull-down experiments using immobilized Nrx-1α and Nrx-1β (Ig-Nrx-1α^{SS4-} and Ig-Nrx-1β^{SS4-}) Ig-fusion proteins with mouse synaptosomal fractions revealed that both Ig-Nrx-1α^{SS4-} and Ig-Nrx-1β^{SS4-} effectively captured NL1, but did not bind to CSTs (Figure 7E), supporting the absence of an interaction of Nrx with CSTs. Viewed together, these results suggest that CST-3 requires Nrxs for its presynapse-inducing activities but is indirectly linked to them.

DISCUSSION

Currently, the neural roles of CST-1 have been extensively studied in the brain, showing that CST-1 is localized to both excitatory and inhibitory synapses and forms a tripartite complex with both Mint/X11 adaptor protein and APP, stabilizing intracellular APP metabolism and thereby suppressing Mint/X11-mediated Aβ-secretion (Araki et al., 2003; Vogt et al., 2001). Moreover, CST-1 mediates the transport of axonal APP-containing organelles in a kinesin-1-dependent manner (Konecna et al., 2006; Vagnoni et al., 2012; Vagnoni et al., 2011). Recently, several genetic studies have implicated CST-2 polymorphisms in episodic memory performance, suggesting that CST-2 might regulate cognitive processes in the brain (Papassotiropoulos et al., 2006; Preuschhof et al., 2010). However, the synaptic functions of CST proteins have not been investigated. Particularly, the functions of CST-3 have been less explored than those of CST-1 and CST-2. The cadherin superfamily proteins are key regulators of various neuronal processes, but have been generally considered dispensable for *de novo* synapse formation (Scheiffele et al., 2000; Takeichi, 2007). Instead, these proteins have been suggested as critical for modulating numerous synaptic signaling pathways and synaptic plasticity (Arikkath and Reichardt, 2008). Here, we demonstrated that the two cadherin repeats of CST-3 are required for the synaptogenic activity of this protein (Figure 2). However, it was recently reported that the cadherin repeats of CST-3 are required, but not sufficient, for the synaptogenic activity of CST-3 (Pettem et al., 2013), inconsistent with the results obtained in the present study. Although the nature of this discrepancy is currently unclear, the surface expression levels of the plasmids used in these two studies might differ, leading to completely different conclusions. Moreover, the fact that CSTs possess only two cadherin repeats at the N-terminus is a striking exception in the cadherin superfamily, as the majority of cadherin proteins possess five or more repeats (Hulpiau and van Roy, 2009). Furthermore, CST-TKD halted neuron growth, resulting in smaller soma size (Figures 4 and S6). Although the roles of cadherin superfamily proteins in neuron development have been relatively well established, to our knowledge, this study is the first report that members of this family are directly involved in the neuron soma development. Importantly, CSTs are among a small group of evolutionarily conserved synapse organizers, including NLs, Nrxs, and Leukocyte antigen-related receptor protein tyrosine phosphatases (LAR-RPTPs). In

invertebrates, these synapse organizers have been implicated in neuron development and synaptic functions (Calahorro and Ruiz-Rubio, 2013; Hu et al., 2012). CASY-1, the *C. elegans* ortholog of CSTs, is also essential for associative learning (Hoerndli et al., 2009; Ikeda et al., 2008); the Drosophila ortholog of CSTs (Cals) has not yet been functionally explored. Because the neuronal expression of human CST-2 in *C. elegans* functionally rescues the learning defects of CASY-1 mutants, we also examined whether Cals is synaptogenic using heterologous synapse-formation assays. However, Cals proteins, such as CST-1 or CST-2, did not induce presynaptic differentiation (**data not shown**). Thus, whether the functional significance of the Nrx/CST interaction reported in the present study also applies to the other model organisms remains undetermined.

Nrxs are essential for synapse formation and function (reviewed in Craig and Kang, 2007; Sudhof, 2008). The coupling of calcium channels to presynaptic machinery in mouse genetics studies has shown that α-Nrxs are important for presynaptic functions, but not structural integrity (Dudanova et al., 2007; Missler et al., 2003). The loss of all three α-Nrxs dramatically reduces spontaneous and evoked synaptic transmission at both excitatory and inhibitory synapses, although the defect in excitatory synaptic transmission reflects an Nrx-α1 deficiency (Etherton et al., 2009; Missler et al., 2003). α-Nrxs *trans*-synaptically interacts with a multitude of postsynaptic adhesion molecules, including NLs, LRRTMs, cerebellins, dystroglycans, latrophilins, and neurexophilins (reviewed in (Krueger et al., 2012)). However, because most of these postsynaptic ligands interact with both α- and β-Nrxs (except neurexophilins), the functions of these synaptic adhesion pathways cannot be exclusively attributed to α-Nrx-specific synaptic functions. The data obtained in the present study suggest that CST-3 does not form a physical complex with Nrxs, but requires interactions with these molecules for synaptogenic activities, suggesting unidentified ‘intermediary’ proteins that bridge CST-3 and Nrxs. A recent study reported that α-Nrxs, but not β-Nrxs, directly interact with CST-3 (Pettem et al., 2013). These authors presented a series of cell surface-labeling and pull-down assays to demonstrate the interaction of CST-3 with α-Nrxs. However, we did not observe any significant binding of CST-3 to any of the three α-Nrxs in cell surface-labeling assays (Figure 7). Moreover, we found that various deletion variants of Nrx-1α did not interact with CST-3. Furthermore, we did not observe any significant enrichment of CSTs with recombinant Nrx-1α proteins in mouse brain pull-down assays (Figure 7). Overall, we found no clear-cut evidence to support the direct interaction of CST-3 with α-Nrxs. Nevertheless, we observed that Nrxs are essential for CST-3 function because the triple-knockdown of Nrxs significantly reduced the synaptogenic activities of CST-3 (Figure 6). Currently, there is no precise explanation for the discrepant results between the two papers. Indeed, our data present two inherent paradoxes that we cannot at present resolve, but that paint a very different picture than that proposed by Pettem et al. First, in artificial synapse-formation assays only CST-3 is active, but not the other CSTs, whereas only a combined triple knockdown of all CSTs affects synapse density. Second, in pull-downs with recombinant CST-3 some Nrxs were found and in artificial synapse-formation assays the presynaptic Nrx-TKD blocked CST-3-induced synapse formation, but in all other binding assays, no CST-3 binding to Nrxs was detected. Most of these data were obtained in our laboratories before the Pettem et al. was published but we did not proceed to publication because we could not rationally reconcile these results

and formulate a coherent conclusion from them. We do feel, however, that based on our observations it is highly unlikely that CSTs are general Nrx ligands analogous to LRRTMs, neuroligins, or cerebellins.

In the present study, we found that the suppression of multiple CST isoforms, but not individual CSTs, reduced synapse density, suggesting redundancy among CST isoforms (Figure 4). However, electrophysiology experiments in both cultured and *in vivo* neurons indicated that CSTs act preferentially to inhibitory synapse structure and function (Figures 5 and S5). These results are consistent with those from previous reports, showing that triple NL loss through acute KD in cultured neurons suppresses the frequency of mIPSCs (Chih et al., 2005). Moreover, α-Nrx-specific sequences confer specific activity toward inhibitory synapses in heterologous synapse formation-assays (Kang et al., 2008), suggesting that CST-3 might be a major postsynaptic mediator of inhibitory synapse organization through α-Nrxs. Notably, although CST-3 KD alone did not significantly affect synapse density in cultured neurons (Figure 4), synaptic transmission might be impaired at specific synapses, as demonstrated for individual NL isoforms (Chubykin et al., 2007). Consistently, analyses of CST-3-KO mice showed that both excitatory and inhibitory synaptic transmission are impaired (Pettem et al., 2013).

Although certain mechanistic details remain unresolved, CSTs have been predominantly associated with AD pathogenesis (reviewed in (Suzuki et al., 2006)). For example, CST-1 modulates the effects of APP processing and trafficking, and CSTs co-accumulate with APP in dystrophic neuritis. Moreover, CST-1 KD perturbs the axonal transport of APP-containing vesicles and alters APP processing, leading to increased Aβ production (Vagnoni et al., 2012). Furthermore, the proteolytically processed C-terminal fragment of CST-3 (CTF) accumulates in dystrophic neurites surrounding Aβ plaques in AD model mice, accelerating neuronal death (Uchida et al., 2013). Intriguingly, CST-1 and CST-3 have been identified as potential biomarkers of AD (Ringman et al., 2012; Yin et al., 2009). Recently, several γ-secretase mutations impair Nrx-3β processing, linking Nrxs with AD pathogenesis (Bot et al., 2011). It is tempting to speculate that the misregulation of CST-3 and/or Nrx proteolytic processing might induce a subset of early-onset familial AD. It has been suggested that an imbalance between excitatory and inhibitory synapses is the central mechanism underlying a multitude of neuropsychiatric disorders. In the present study, we observed that inhibitory synapse function is selectively disrupted through CST-TKD in both cultured and *in vivo* neurons. Although there are currently no reports that CSTs are involved in neuropsychiatric disorders, it is likely that the synaptic dysfunction of CSTs contributes to the pathogenesis of multiple neuropsychiatric disorders. Intriguingly, CST-1 mRNA levels are upregulated in chronic cocaine-treated mice, suggesting that CST-1 dysfunction might be associated with addiction (Yao et al., 2004) via impaired long-term synaptic plasticity at inhibitory synapses (Niehaus et al., 2010). Some neuropsychiatric disorders (e.g., schizophrenia, autism, and intellectual disabilities) has been associated with specific defects in the development and function of interneurons. Considering that CST-2 and CST-3 are highly expressed in interneurons (Hintsch et al., 2002), it is possible that the molecular dysfunctions of these CST isoforms contribute to these diseases.

In conclusion, we identified CST-3 as a synaptogenic adhesion molecule that forms complexes with Nrxs. Future studies should identify 'intermediary' protein(s) that functionally bridge CST-3 and Nrxs, characterize the detailed molecular mechanisms underlying the intracellular transduction of CST-3/Nrxs extracellular signals, identify the presynaptic receptors for CST-1 and/or CST-2 to establish a complete understanding of the synaptic functions of CST proteins, and validate the functions of CSTs proposed in the current study *in vivo*.

EXPERIMENTAL PROCEDURES

The Construction of Expression Vectors

HA-CSTs encode full-length mouse CSTs containing an inserted HA-epitope. The signal peptide sequence of CST-1 (amino acids [aa] 1–28) was initially PCR-amplified, digested with *Hin*dIII/*Bgl*II, and cloned into the GW1 vector (British Biotechnology). The remaining of CST-1 sequences (aa 29–979) were PCR-amplified, digested with *Bgl*II and *Eco*RI, and cloned into the GW1 vector. Full-length CST-2 and CST-3, excluding the corresponding signal peptide sequences (CST-2, aa 21–966; CST-3, aa 20–956), were PCR-amplified, digested with *Xma*I and *Sac*II, and subcloned into the pDisplay vector (Invitrogen). pDis-CST-3 deletion variants encode the indicated CST-3 fragment (Cad+LNS, aa 36–541; LNS +linker, aa 335–846; Cad repeats, aa 20–257; LNS, aa 335–541; Cad repeat 1, aa 36–158; and Cad repeat 2, aa 152–259) cloned into the pDisplay vector at *Xma*I and *Sac*II sites. pDis-Nrxs encode the indicated Nrx-1α, Nrx-1β, Nrx-2α, or Nrx-3α fragments cloned into the pDisplay vector at the indicated restriction enzyme sites. To construct shRNA lentiviral expression vectors, oligonucleotides targeting mouse CST-1, CST-2, or CST-3 were annealed, phosphorylated, and cloned into the *Xho*I and *Xba*I sites of a single KD vector (L-309 vector; see Figure 4A for a schematic diagram of vectors) immediately downstream of the human H1 promoter. For CST-TKD, oligonucleotides targeting CST-1 (J73), CST-2 (J76), and CST-3 (J81) were subcloned respectively into the *Xho*I-*Xba*I (J73), *Bst*EII-*Bsi*WI (J76), and *Sbf*I-*Bst*BI (J81) sites of a TKD vector (L-313 vector) containing two human H1 promoters and two human U6 promoters. For the details, see Extended Experimental Procedures.

Antibodies

used in this study are described in detail in the Supplemental materials associated with this paper.

Heterologous Synapse-formation Assays, Cell Surface-labeling Assays, and Cell-adhesion Assays

were performed using HEK293T cells as previously described (Ko et al., 2009a)

Affinity Chromatography and Mass Spectroscopy

were performed using recombinant CST-3 fusion proteins as previously described (Ko et al., 2009a).

Production of Recombinant Lentiviruses

Recombinant lentiviruses were produced through the transfection of human embryonic kidney 293T cells with four plasmids—L-313 vectors (L-313-Nrx-TKD or L-313 alone), pRRE, pVSVg, and pREV—using FuGENE-6 (Roche) as previously described (Ko et al., 2011).

Primary Neuronal Culture, Transfections, Immunocytochemistry, Image Acquisition and Analyses

were performed using E18-derived mouse hippocampal cultured neurons and confocal microscopy as previously described (Ko et al., 2009b).

In Utero Electroporation

Pregnant ICR mice at 15 days post coitum (d.p.c) were anesthetized with an intraperitoneal injection of pentobarbital sodium, and the uterine horns were exposed through a longitudinal incision in the abdomen. Approximately 1 μl of DNA solution containing 1 mg/ml pCAGGS-EGFP, 1.5 mg/ml L-315-CST-TKD shRNA, and 0.01% Fast Green in PBS or 1 mg/ml pCAGGS-EGFP, 1.5 mg/ml L-315 control shRNA, and 0.01% Fast Green in PBS, was injected into the lateral ventricle of each embryo through a glass capillary electrode. The uteri were returned to the peritoneal cavity, and the incisions were sutured. The operated mice were returned to their home cages and subsequently allowed to deliver naturally. The transfected pups were identified at P_0 by visualizing the GFP signals through the scalp using an LED penlight (Handy Blue; Reryon).

Electrophysiology

Cell culture and slice electrophysiology were performed as previously described (Ko et al., 2011).

Statistics

All data are expressed as the means ± SEM. All experiments were performed with at least three independent cultures and statistically evaluated using Student's t-test and one-way ANOVA, with cell numbers as the basis for 'n'.

Further details available in the Extended Experimental Procedures.

Supplementary Material

Refer to Web version on PubMed Central for supplementary material.

ACKNOWLEDGMENTS

The authors would like to thank Dr. Peter Sonderegger (University of Zurich, Switzerland) for kindly providing the CST expression vectors and Minsoo Kang for assistance with the quantitative analyses. This work was supported by the Korea Healthcare Technology R&D Project through the Ministry for Health & Welfare Affairs, Republic of Korea (A120590 and A120723 to J.K.), Basic Science Research Program through the National Research Foundation of Korea (NRF) funded by the Ministry of Education, Science and Technology (NRF-2013R1A6A3A04061338 to J.W.U.), Brain Research Program through the National Research Foundation of Korea (NRF) funded by the Ministry of Science, ICT & Future Planning (2013-035006 to H.K.), National Research Foundation of Korea (NRF), Ministry of Education, Science and Technology (2008-0061888 and KRF-2008-313-

E00075 to K.S.P.), JST PRESTO (to K.T.), JSPS KAKENHI (Grant numbers 25282242, 24650183, and 23650180 to K.T.), and the Takeda Science Foundation (to K.T.).

REFERENCES

Araki Y, Kawano T, Taru H, Saito Y, Wada S, Miyamoto K, Kobayashi H, Ishikawa HO, Ohsugi Y, Yamamoto T, et al. The novel cargo Alcadein induces vesicle association of kinesin-1 motor components and activates axonal transport. The EMBO journal. 2007; 26:1475–1486. [PubMed: 17332754]

Araki Y, Tomita S, Yamaguchi H, Miyagi N, Sumioka A, Kirino Y, Suzuki T. Novel cadherin-related membrane proteins, Alcadeins, enhance the X11-like protein-mediated stabilization of amyloid beta-protein precursor metabolism. The Journal of biological chemistry. 2003; 278:49448–49458. [PubMed: 12972431]

Arikkath J, Reichardt LF. Cadherins and catenins at synapses: roles in synaptogenesis and synaptic plasticity. Trends in neurosciences. 2008; 31:487–494. [PubMed: 18684518]

Biederer T, Scheiffele P. Mixed-culture assays for analyzing neuronal synapse formation. Nature protocols. 2007; 2:670–676.

Bot N, Schweizer C, Ben Halima S, Fraering PC. Processing of the synaptic cell adhesion molecule neurexin-3beta by Alzheimer disease alpha- and gamma-secretases. The Journal of biological chemistry. 2011; 286:2762–2773. [PubMed: 21084300]

Calahorro F, Ruiz-Rubio M. Human alpha- and beta-NRXN1 isoforms rescue behavioral impairments of Caenorhabditis elegans neurexin-deficient mutants. Genes, brain, and behavior. 2013; 12:453–464.

Chih B, Engelman H, Scheiffele P. Control of excitatory and inhibitory synapse formation by neuroligins. Science. 2005; 307:1324–1328. [PubMed: 15681343]

Chubykin AA, Atasoy D, Etherton MR, Brose N, Kavalali ET, Gibson JR, Sudhof TC. Activity-dependent validation of excitatory versus inhibitory synapses by neuroligin-1 versus neuroligin-2. Neuron. 2007; 54:919–931. [PubMed: 17582332]

Dudanova I, Tabuchi K, Rohlmann A, Sudhof TC, Missler M. Deletion of alpha-neurexins does not cause a major impairment of axonal pathfinding or synapse formation. The Journal of comparative neurology. 2007; 502:261–274. [PubMed: 17347997]

Etherton MR, Blaiss CA, Powell CM, Sudhof TC. Mouse neurexin-1alpha deletion causes correlated electrophysiological and behavioral changes consistent with cognitive impairments. Proceedings of the National Academy of Sciences of the United States of America. 2009; 106:17998–18003. [PubMed: 19822762]

Gokce O, Sudhof TC. Membrane-tethered monomeric neurexin LNS-domain triggers synapse formation. The Journal of neuroscience : the official journal of the Society for Neuroscience. 2013; 33:14617–14628. [PubMed: 24005312]

Hintsch G, Zurlinden A, Meskenaite V, Steuble M, Fink-Widmer K, Kinter J, Sonderegger P. The calsyntenins--a family of postsynaptic membrane proteins with distinct neuronal expression patterns. Molecular and cellular neurosciences. 2002; 21:393–409. [PubMed: 12498782]

Hoerndli FJ, Walser M, Frohli Hoier E, de Quervain D, Papassotiropoulos A, Hajnal A. A conserved function of C. elegans CASY-1 calsyntenin in associative learning. PloS one. 2009; 4:e4880. [PubMed: 19287492]

Hu Z, Hom S, Kudze T, Tong XJ, Choi S, Aramuni G, Zhang W, Kaplan JM. Neurexin and neuroligin mediate retrograde synaptic inhibition in C. elegans. Science. 2012; 337:980–984. [PubMed: 22859820]

Hulpiau P, van Roy F. Molecular evolution of the cadherin superfamily. The international journal of biochemistry & cell biology. 2009; 41:349–369. [PubMed: 18848899]

Ikeda DD, Duan Y, Matsuki M, Kunitomo H, Hutter H, Hedgecock EM, Iino Y. CASY-1, an ortholog of calsyntenins/alcadeins, is essential for learning in Caenorhabditis elegans. Proceedings of the National Academy of Sciences of the United States of America. 2008; 105:5260–5265. [PubMed: 18381821]

Kang Y, Zhang X, Dobie F, Wu H, Craig AM. Induction of GABAergic postsynaptic differentiation by alpha-neurexins. The Journal of biological chemistry. 2008; 283:2323–2334. [PubMed: 18006501]

Ko J, Fuccillo MV, Malenka RC, Sudhof TC. LRRTM2 functions as a neurexin ligand in promoting excitatory synapse formation. Neuron. 2009a; 64:791–798. [PubMed: 20064387]

Ko J, Soler-Llavina GJ, Fuccillo MV, Malenka RC, Sudhof TC. Neuroligins/LRRTMs prevent activity- and Ca2+/calmodulin-dependent synapse elimination in cultured neurons. The Journal of cell biology. 2011; 194:323–334. [PubMed: 21788371]

Ko J, Zhang C, Arac D, Boucard AA, Brunger AT, Sudhof TC. Neuroligin-1 performs neurexin-dependent and neurexin-independent functions in synapse validation. The EMBO journal. 2009b; 28:3244–3255. [PubMed: 19730411]

Konecna A, Frischknecht R, Kinter J, Ludwig A, Steuble M, Meskenaite V, Indermuhle M, Engel M, Cen C, Mateos JM, et al. Calsyntenin-1 docks vesicular cargo to kinesin-1. Molecular biology of the cell. 2006; 17:3651–3663. [PubMed: 16760430]

Krueger DD, Tuffy LP, Papadopoulos T, Brose N. The role of neurexins and neuroligins in the formation, maturation, and function of vertebrate synapses. Current opinion in neurobiology. 2012; 22:412–422. [PubMed: 22424845]

Maruta C, Saito Y, Hata S, Gotoh N, Suzuki T, Yamamoto T. Constitutive cleavage of the single-pass transmembrane protein alcadeinalpha prevents aberrant peripheral retention of Kinesin-1. PloS one. 2012; 7:e43058. [PubMed: 22905201]

Missler M, Sudhof TC, Biederer T. Synaptic cell adhesion. Cold Spring Harbor perspectives in biology. 2012; 4:a005694. [PubMed: 22278667]

Missler M, Zhang W, Rohlmann A, Kattenstroth G, Hammer RE, Gottmann K, Sudhof TC. Alpha-neurexins couple Ca2+ channels to synaptic vesicle exocytosis. Nature. 2003; 423:939–948. [PubMed: 12827191]

Niehaus JL, Murali M, Kauer JA. Drugs of abuse and stress impair LTP at inhibitory synapses in the ventral tegmental area. The European journal of neuroscience. 2010; 32:108–117. [PubMed: 20608969]

Papassotiropoulos A, Stephan DA, Huentelman MJ, Hoerndli FJ, Craig DW, Pearson JV, Huynh KD, Brunner F, Corneveaux J, Osborne D, et al. Common Kibra alleles are associated with human memory performance. Science. 2006; 314:475–478. [PubMed: 17053149]

Pettem KL, Yokomaku D, Luo L, Linhoff MW, Prasad T, Connor SA, Siddiqui TJ, Kawabe H, Chen F, Zhang L, et al. The Specific alpha-Neurexin Interactor Calsyntenin-3 Promotes Excitatory and Inhibitory Synapse Development. Neuron. 2013; 80:113–128. [PubMed: 24094106]

Pettitt, J. The cadherin superfamily. WormBook: the online review of C elegans biology; 2005. p. 1-9.

Preuschhof C, Heekeren HR, Li SC, Sander T, Lindenberger U, Backman L. KIBRA and CLSTN2 polymorphisms exert interactive effects on human episodic memory. Neuropsychologia. 2010; 48:402–408. [PubMed: 19804789]

Ringman JM, Schulman H, Becker C, Jones T, Bai Y, Immermann F, Cole G, Sokolow S, Gylys K, Geschwind DH, et al. Proteomic changes in cerebrospinal fluid of presymptomatic and affected persons carrying familial Alzheimer disease mutations. Archives of neurology. 2012; 69:96–104. [PubMed: 22232349]

Scheiffele P, Fan J, Choih J, Fetter R, Serafini T. Neuroligin expressed in nonneuronal cells triggers presynaptic development in contacting axons. Cell. 2000; 101:657–669. [PubMed: 10892652]

Sudhof TC. Neuroligins and neurexins link synaptic function to cognitive disease. Nature. 2008; 455:903–911. [PubMed: 18923512]

Sugita S, Saito F, Tang J, Satz J, Campbell K, Sudhof TC. A stoichiometric complex of neurexins and dystroglycan in brain. The Journal of cell biology. 2001; 154:435–445. [PubMed: 11470830]

Suzuki T, Araki Y, Yamamoto T, Nakaya T. Trafficking of Alzheimer's disease-related membrane proteins and its participation in disease pathogenesis. Journal of biochemistry. 2006; 139:949–955. [PubMed: 16788045]

Takeichi M. The cadherin superfamily in neuronal connections and interactions. Nature reviews Neuroscience. 2007; 8:11–20.

Uchida Y, Gomi F, Murayama S, Takahashi H. Calsyntenin-3 C-terminal fragment accumulates in dystrophic neurites surrounding abeta plaques in tg2576 mouse and Alzheimer disease brains: its neurotoxic role in mediating dystrophic neurite formation. The American journal of pathology. 2013; 182:1718–1726. [PubMed: 23499467]

Ullrich B, Ushkaryov YA, Sudhof TC. Cartography of neurexins: more than 1000 isoforms generated by alternative splicing and expressed in distinct subsets of neurons. Neuron. 1995; 14:497–507. [PubMed: 7695896]

Um JW, Ko J. lLAR-RPTPs: synaptic adhesion molecules that shape synapse development. Trends in cell biology. 2013

Vagnoni A, Perkinton MS, Gray EH, Francis PT, Noble W, Miller CC. Calsyntenin-1 mediates axonal transport of the amyloid precursor protein and regulates Abeta production. Human molecular genetics. 2012; 21:2845–2854. [PubMed: 22434822]

Vagnoni A, Rodriguez L, Manser C, De Vos KJ, Miller CC. Phosphorylation of kinesin light chain 1 at serine 460 modulates binding and trafficking of calsyntenin-1. Journal of cell science. 2011; 124:1032–1042. [PubMed: 21385839]

Vogt L, Schrimpf SP, Meskenaite V, Frischknecht R, Kinter J, Leone DP, Ziegler U, Sonderegger P. Calsyntenin-1, a proteolytically processed postsynaptic membrane protein with a cytoplasmic calcium-binding domain. Molecular and cellular neurosciences. 2001; 17:151–166. [PubMed: 11161476]

Yao WD, Gainetdinov RR, Arbuckle MI, Sotnikova TD, Cyr M, Beaulieu JM, Torres GE, Grant SG, Caron MG. Identification of PSD-95 as a regulator of dopamine-mediated synaptic and behavioral plasticity. Neuron. 2004; 41:625–638. [PubMed: 14980210]

Yim YS, Kwon Y, Nam J, Yoon HI, Lee K, Kim DG, Kim E, Kim CH, Ko J. Slitrks control excitatory and inhibitory synapse formation with LAR receptor protein tyrosine phosphatases. Proceedings of the National Academy of Sciences. 2013; 110:4057–4062.

Yin GN, Lee HW, Cho JY, Suk K. Neuronal pentraxin receptor in cerebrospinal fluid as a potential biomarker for neurodegenerative diseases. Brain research. 2009; 1265:158–170. [PubMed: 19368810]

Highlights

- CST-3 specifically induces presynaptic differentiation
- CSTs are required for inhibitory synapse structure and function
- CST-3 requires Nrxs as functional receptors for presynaptic development
- CST-3 does not directly interact with Nrxs

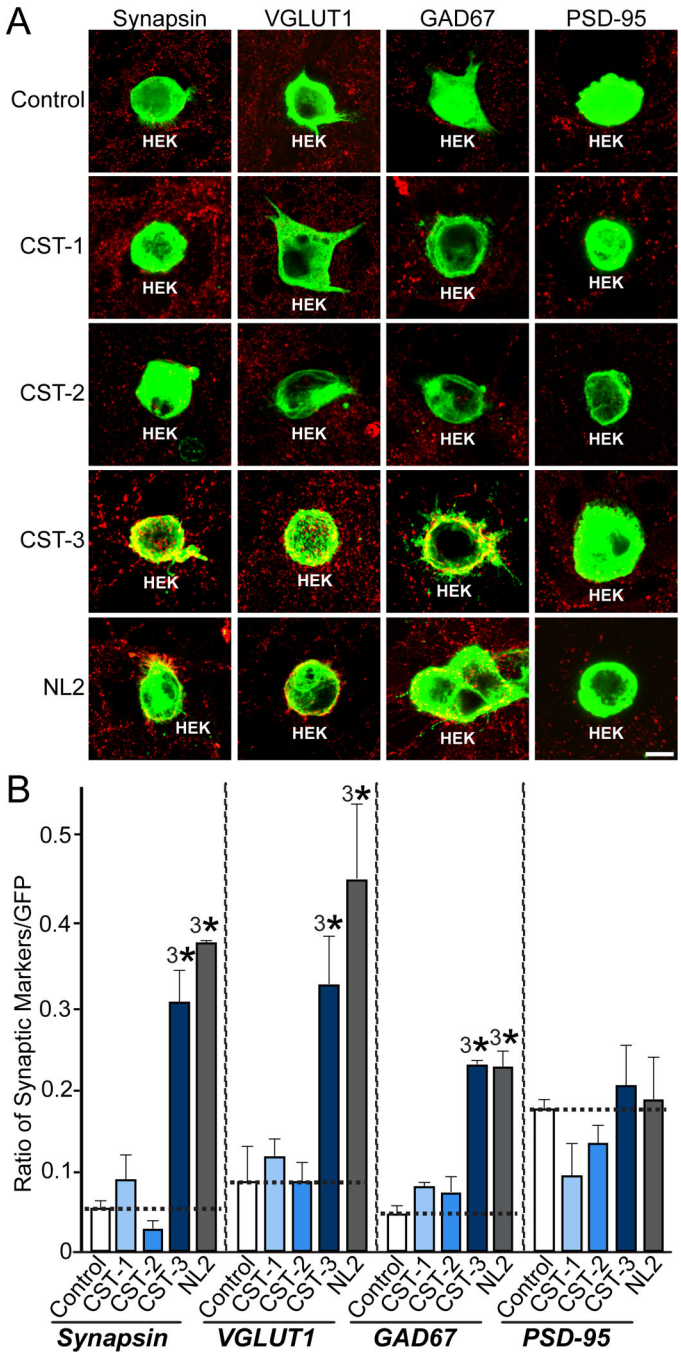

Figure 1. CST-3 Induces Presynaptic Differentiation in Heterologous Synapse-formation Assays

(**A**) CST-3 promotes the formation of excitatory and inhibitory presynapses in heterologous synapse-formation assays. Rat hippocampal neurons were cocultured for 3 d (DIV10-13) with HEK293T cells expressing EGFP alone (control) or coexpressing EGFP and N-terminally HA-tagged CST-1 extracellular fragment (CST-1), CST-2 extracellular fragment (CST-2), CST-3 extracellular fragment (CST-3), or an mVenus-fusion protein of neuroligin-2 (NL2). The panels show representative immunofluorescence images of cocultures stained with antibodies to EGFP (green) and various presynaptic (VGLUT1,

GAD67) and postsynaptic (PSD-95) markers (red). Coincident green and red signals are shown in yellow. Scale bar = 20 μm (applies to all images).(**B**) Quantitation of the heterologous synapse-formation activity of CST-1, CST-2, CST-3, and NL2. To quantify the experiments described in (**A**), the ratio of the synaptic marker staining to EGFP fluorescence (from absolute red and green fluorescence values) was measured. All data are shown as means ± SEMs (^{3}*$p<0.001$, assessed using analysis of variance [ANOVA] with Tukey's test; "n" denotes the total number of HEK293T cells analyzed, as follows: Control/synapsin, n=18; CST-1/synapsin, n=21; CST-2/synapsin, n=17; CST-3/synapsin, n=16; NL2/synapsin, n=14; Control/VGLUT1, n=22; CST-1/VGLUT1, n=17; CST-2/VGLUT1, n=15; CST-3/VGLUT1, n=15; NL2/VGLUT1, n=16; Control/GAD67, n=15; CST-1/GAD67, n=15; CST-2/GAD67, n=14; CST-3/GAD67, n=15; NL2/GAD67, n=14; Control/PSD-95, n=15; CST-1/PSD-95, n=16; CST-2/PSD-95, n=17; CST-3/PSD-95, n=16; and NL2/PSD-95, n=15).

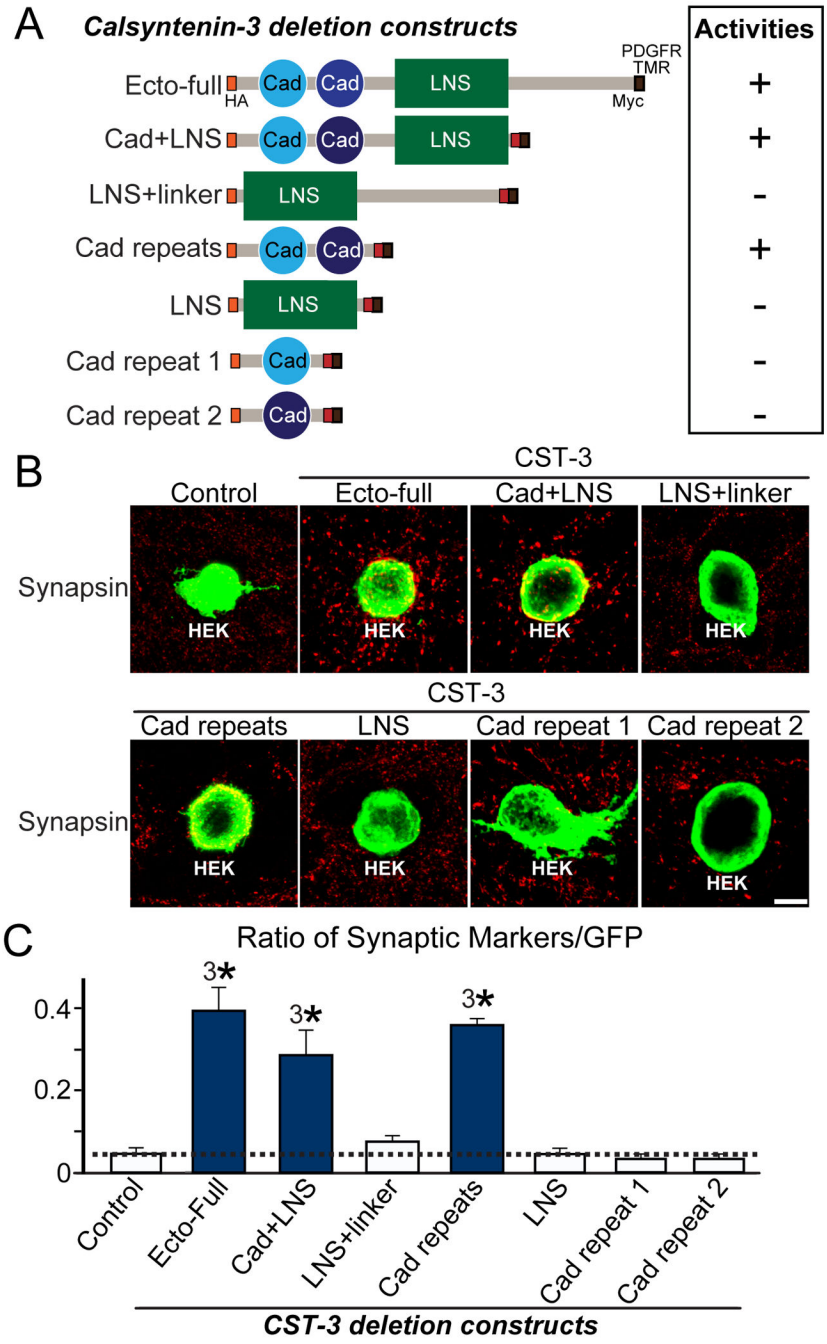

Figure 2. N-terminal Cadherin Repeats Are Required for the Synaptogenic Activities of CST-3

(**A**) Diagrams of the CST-3 variants used in heterologous synapse-formation assays. The full extracellular region of CST-3 (Ecto-full) carrying an HA epitope inserted after the signal peptide sequence was cloned into the pDisplay vector. CST-3 fragments carrying the following extracellular regions were also prepared as pDisplay vectors: Cad+LNS, a CST-3 fragment containing cadherin repeats and an LNS domain; LNS+linker, a CST-3 fragment containing the LNS domain and the linker region between an LNS domain and a transmembrane segment; Cad repeats, a CST-3 fragment containing two cadherin repeats;

LNS, a CST-3 fragment containing the LNS domain; Cad repeat 1, a CST-3 fragment containing the first cadherin repeat; and Cad repeat 2, a CST-3 fragment containing the second cadherin repeat. (**B–C**) Synaptogenic activity of various CST-3 constructs (described in [**A**]) in heterologous synapse formation-assays. Representative immunofluorescence images of cocultures stained with antibodies to HA (green) and synapsin (red). Coincident signals are shown in yellow. Scale bar = 20 μm (applies to all images) (**B**). Quantitation of heterologous synapse-formation assays (**C**), measured as the ratio of synapsin to HA fluorescence signals. The dashed lines correspond to Control values, used as the baseline. The data are shown as the means ± SEMs (^{3}*$p<0.001$, assessed using analysis of variance [ANOVA] with Tukey's test; "n" denotes the total number of HEK293T cells analyzed, as follows: Control, n=15; Ecto-Full, n=17; Cad+LNS, n=17; LNS+linker, n=16; Cad repeats, n=14; LNS, n=15; Cad repeat 19, n=16; and Cad repeat 2, n=16).

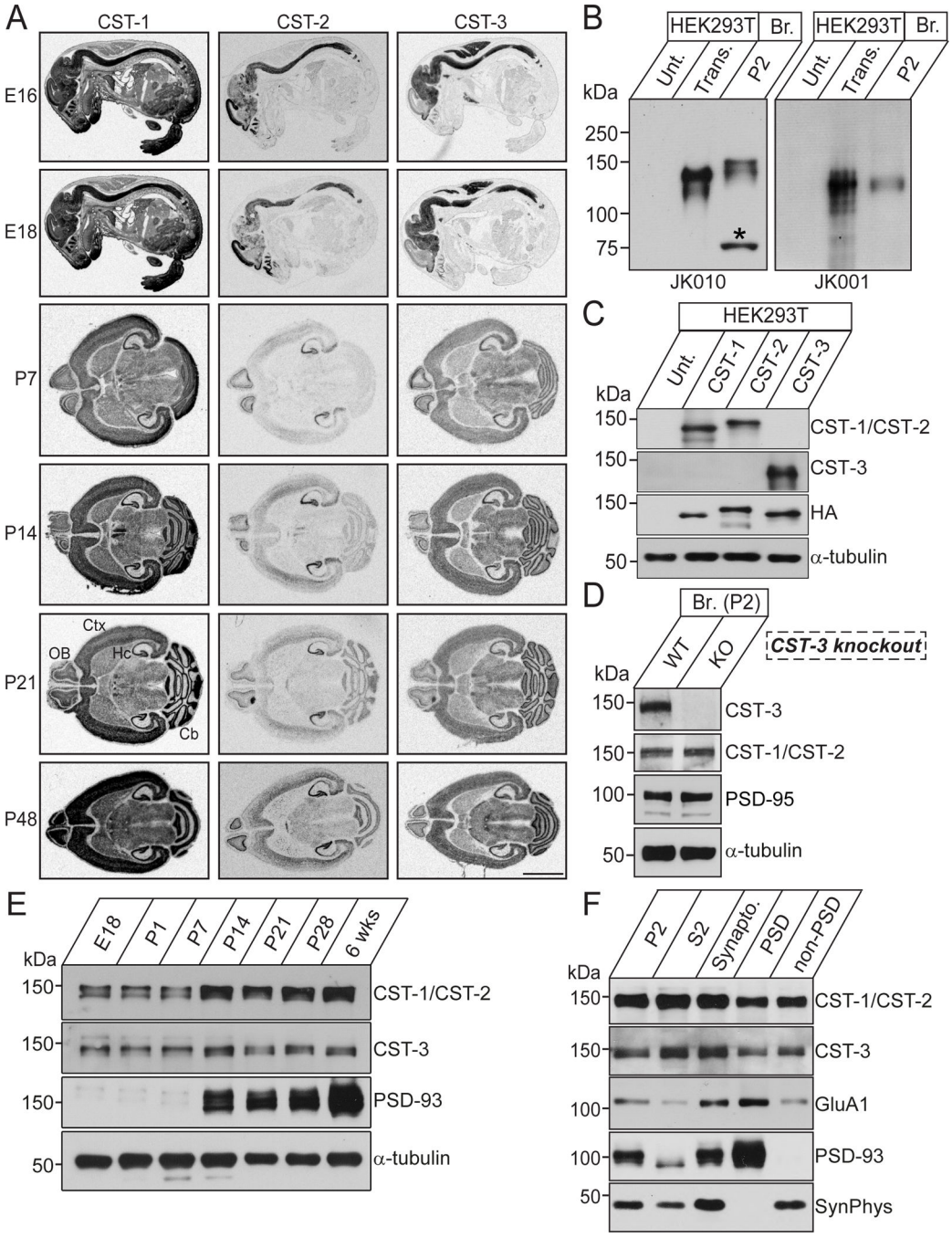

Figure 3. Expressions of CSTs in Mouse Brains

(**A**) CST mRNA distribution patterns in the developing and adult mouse brains. Sections from E16, E18, P7, P14, P21, and P48 (adult) mouse brains were probed with CST-1, CST-2, and CST-3 cRNAs. Scale bar = 5 mm. Cb, cerebellum; Ctx, cerebral cortex; Hc, hippocampus; OB, olfactory bulb. (**B**) Biochemical characterization of the CST antibodies used in this study. Immunoblot analyses of CST antibodies using mouse brain synaptosomes and lysates from HEK293T cells, untransfected or transfected with CST-2 or CST-3 expression vector. JK010 is reactive to both CST-1 and CST-2 proteins, whereas JK001 is

specific to CST-3. Br., brain; P2, crude synaptosomes; Unt., untransfected HEK293T cell lysates. (**C**) Cross-reactivity of the CST antibodies. HEK293T cells, untransfected or transfected with the indicated CST expression vectors, were immunoblotted with anti-CST-1/CST-2 (JK010) and anti-CST-3 (JK001) antibodies. The expression of HA-tagged CST vectors was confirmed through immunoblotting with anti-HA antibodies. An anti-α-tubulin antibody was used for normalization. (**D**) Authenticity of the anti-CST-3 antibody (JK001). P2 fractions from brains of wild-type or CST-3-KO mice were subjected to immunoblot analyses with the indicated antibodies. An anti-α-tubulin antibody was used for normalization. (**E**) The expression of CST proteins during development. E, embryonic day; P, postnatal day. An anti-α-tubulin antibody was used for normalization. (**F**) Localization of CST proteins in PSD fractions. The proteins from each mouse brain fraction (5 μg) were subjected to immunoblotting with the indicated antibodies. P2, crude synaptosomal fraction; S2, cytosolic and light membrane fraction; PSD, postsynaptic density fraction; SynPhys, synaptophysin; Synapto. Fraction, Synaptosomal fraction.

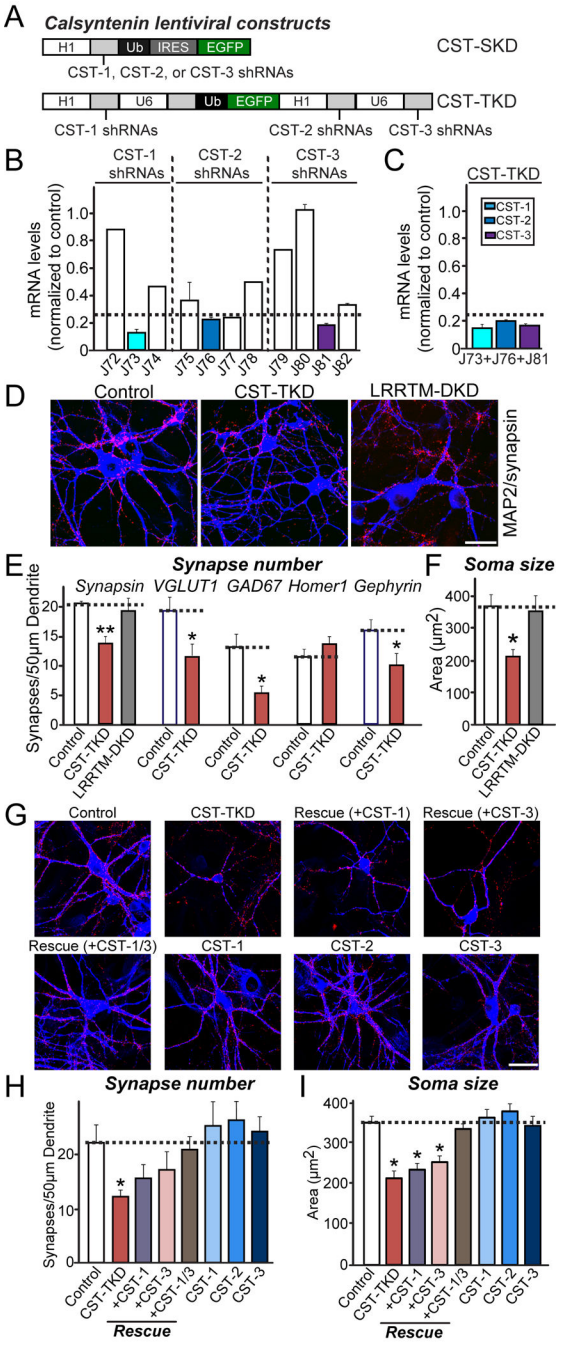

Figure 4. Knockdown of All Three CSTs, but Not Individual CST Isoform Alone, Reduces Synapse Density and Soma Size in Cultured Neurons

(**A**) Schematic diagram of lentiviral shRNA vectors for KD of single CST isoforms (denoted CST-SKD) or triple KD of CST-1 to CST-3 (denoted CST-TKD). (**B**) KD efficacies of shRNA lentiviruses. Levels of target CST mRNAs (CST-1 to CST-3) were measured by quantitative RT-PCR in cultured mouse cortical neurons infected at DIV3 with lentiviruses expressing the indicated shRNAs. The mRNAs were prepared at DIV12-13. The dotted line represents the 75% KD cutoff level for tests of biological effects. (**C**) Measurements of target mRNA levels (CST-1, CST-2, and CST-3) in cultured cortical neurons as described in

(**B**), except that neurons were infected with CST-TKD lentiviruses expressing shRNAs targeting CST-1, CST-2, and CST-3 [described in (**A**)]. The target mRNA measured is colored coded as indicated on the upper right. Dotted line represents the 75% KD cutoff level for tests of biological effects. (**D**) Representative images of cultured hippocampal neurons infected at DIV3 with lentiviruses expressing EGFP alone (control); coexpressing EGFP with shRNAs against CST-1, CST-2, and CST-3 (CST-TKD); or coexpressing EGFP with shRNAs against LRRTM1 and LRRTM2 (LRRTM-DKD). Neurons were analyzed through double immunofluorescence labeling for MAP2 (blue) and synapsin (red) at DIV14. Scale bar = 35 μm (applies to all images). (**E–F**) Summary graphs of the effects of CST-TKD in neurons on synapse density (**E**) (measured using synapsin as a general synapse marker, VGLUT1 as an excitatory presynaptic marker, GAD67 as an inhibitory presynaptic marker, Homer1 as an excitatory postsynaptic marker, and gephyrin as an inhibitory postsynaptic marker), and soma size (**F**) (measured using MAP2 signals). The data are shown as the means ± SEMs (^{3}*$p<0.001$, assessed using analysis of variance [ANOVA] with Tukey's test; 2–3 dendrites per transfected neuron were analyzed and group-averaged; "n" denotes the total number of neurons analyzed, as follows: Control/synapsin, n=16; CST-TKD/synapsin, n=18; LRRTM-DKD/synapsin, n=15; Control/VGLUT1, n=15; CST-TKD/VGLUT1, n=15; Control/GAD67, n=16; CST-TKD/GAD67, n=15; Control/Homer1, n=18; CST-TKD/Homer1, n=21; Control/Gephyrin, n=22; and CST-TKD/Gephyrin n=22). (**G**) Representative images of cultured hippocampal neurons infected with a vector expressing control lentiviruses (control); a vector expressing shRNA viruses against CST-1, CST-2, and CST-3 (CST-TKD); the CST-TKD vector together with lentiviruses expressing full-length human CST-1 [denoted as Rescue (+CST-1)], full-length human CST-3 [denoted as Rescue (+CST-3)], or both human CST-1 and human CST-3 [denoted as Rescue (+CST-1/3)]; or lentiviruses expressing only full-length human CST-1 (CST-1), full-length human CST-2 (CST-2), or full-length human CST-3 (CST-3). The neurons were analyzed through double immunofluorescence using antibodies to MAP2 (blue) and synapsin (red) at DIV14. Scale bar = 35 μm (applies to all images). (**H–I**) Summary graphs of the effects of the indicated lentiviruses on synapse density (**H**) (measured using synapsin as a general synapse marker, and soma size (**I**) (measured using MAP2 signals). Note that lentiviral expression of CST-3 did not increase synapse density, whereas high-level overexpression of CST-3 by calcium phosphate-mediated transfection significantly increased the synapse density (see Figure S7). The data are shown as the means ± SEMs (^{3}*$p<0.001$, assessed using analysis of variance [ANOVA] with Tukey's test; 2–3 dendrites per transfected neuron were analyzed and group-averaged; "n" denotes the total number of neurons analyzed, as follows: Control, n=19; CST-TKD, n=14; CST-TKD+CST-1 rescue, n=15; CST-TKD+CST-2 rescue, n=16; CST-TKD+CST-3 rescue, n=17; CST-TKD+CST-1/3 rescue, n=16; CST-1, n=15; CST-2, n=22; and CST-3, n=17).

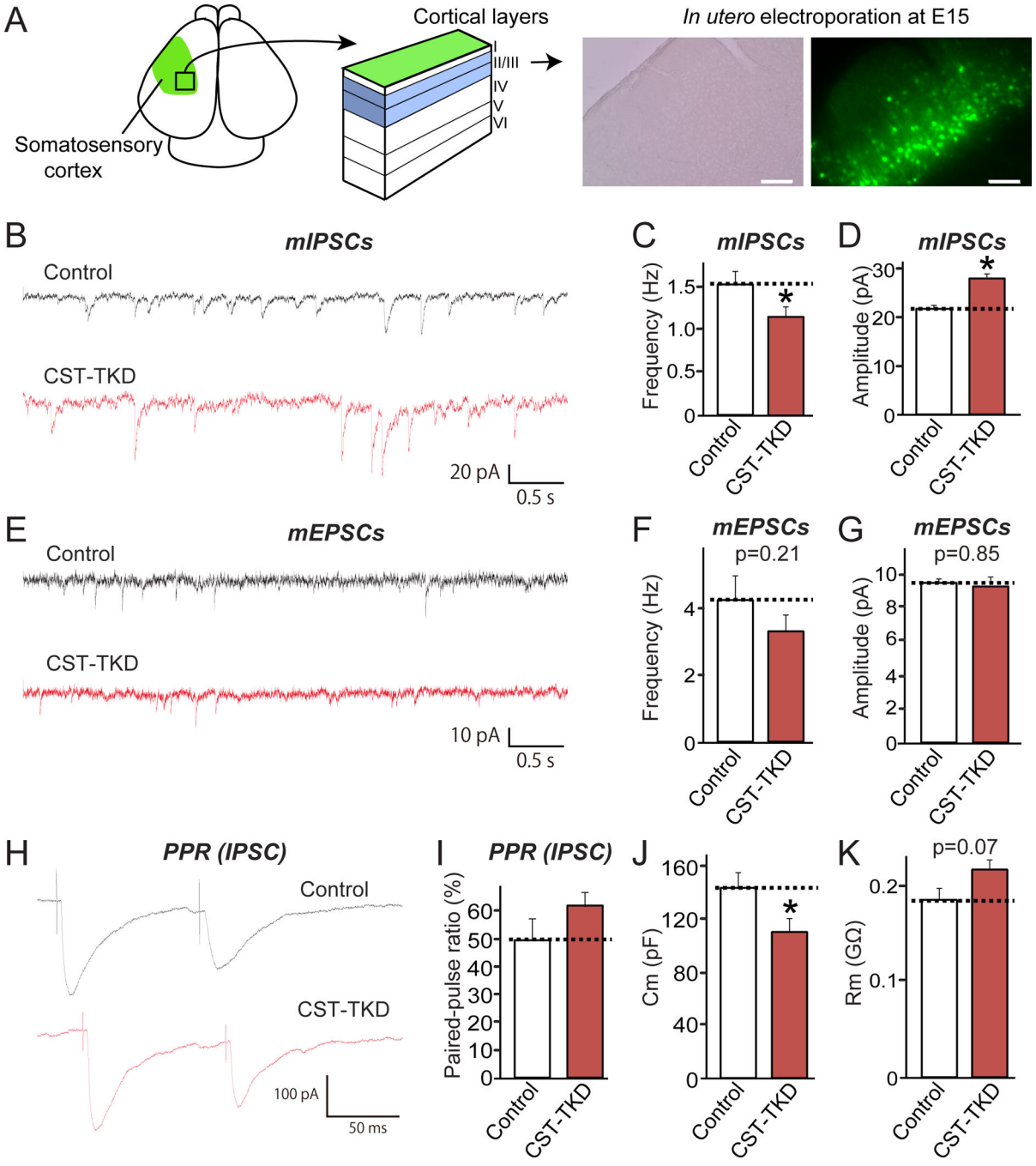

Figure 5. CST Knockdown Impairs Inhibitory, but Not Excitatory, Synaptic Transmission *In Vivo*

(**A**)*In utero* electroporation was performed at E15 to transfect neuron precursors with control or CST-TKD vectors. Coronal brain sections were prepared at P14-19. Many green fluorescence protein (GFP)-positive neurons were detected in layer I I/I II of somatosensory cortex. Scale bar = 250 μm. (**B–D**) Effect of CST proteins on inhibitory synaptic transmission. Representative traces (**B**) of mIPSCs in somatosensory cortical neurons in layer II/III electroporated *in utero* with control or CST-TKD vector. Summary graphs of the

frequencies (**C**) and amplitudes (**D**) of mIPSCs in neurons transfected with control or CST-TKD vectors. (**E–G**) Effect of CST proteins on excitatory synaptic transmission. Representative traces (**e**) of mEPSCs in somatosensory cortical neurons in layer II/III electroporated *in utero* with control or CST-TKD vector. Summary graphs of the frequencies (**F**) and amplitudes (**G**) of mEPSCs in neurons transfected with control or CST-TKD vectors. (**H–I**) Effect of CST proteins on PPR (amplitude of the second IPSC divided by that of the first). Representative traces (**H**) and summary graph (**I**) of PPR measured with 100-ms interstimulus intervals are shown. (**J–K**) Membrane capacitance (j; C_m) and input resistance (k; R_m) measured in control and CST-TKD neurons. The data shown in the panels (**B-K**) represent the means ± SEMs (*$p<0.05$ using Student's *t*-test; "n" denotes the total number of cells recorded, as follows: mIPSC control, n=10; mIPSC CST-TKD, n=12; mEPSC control, n=29; mEPSC CST-TKD, n=30; PPR control, n=13; and PPR CST-TKD, n=15).

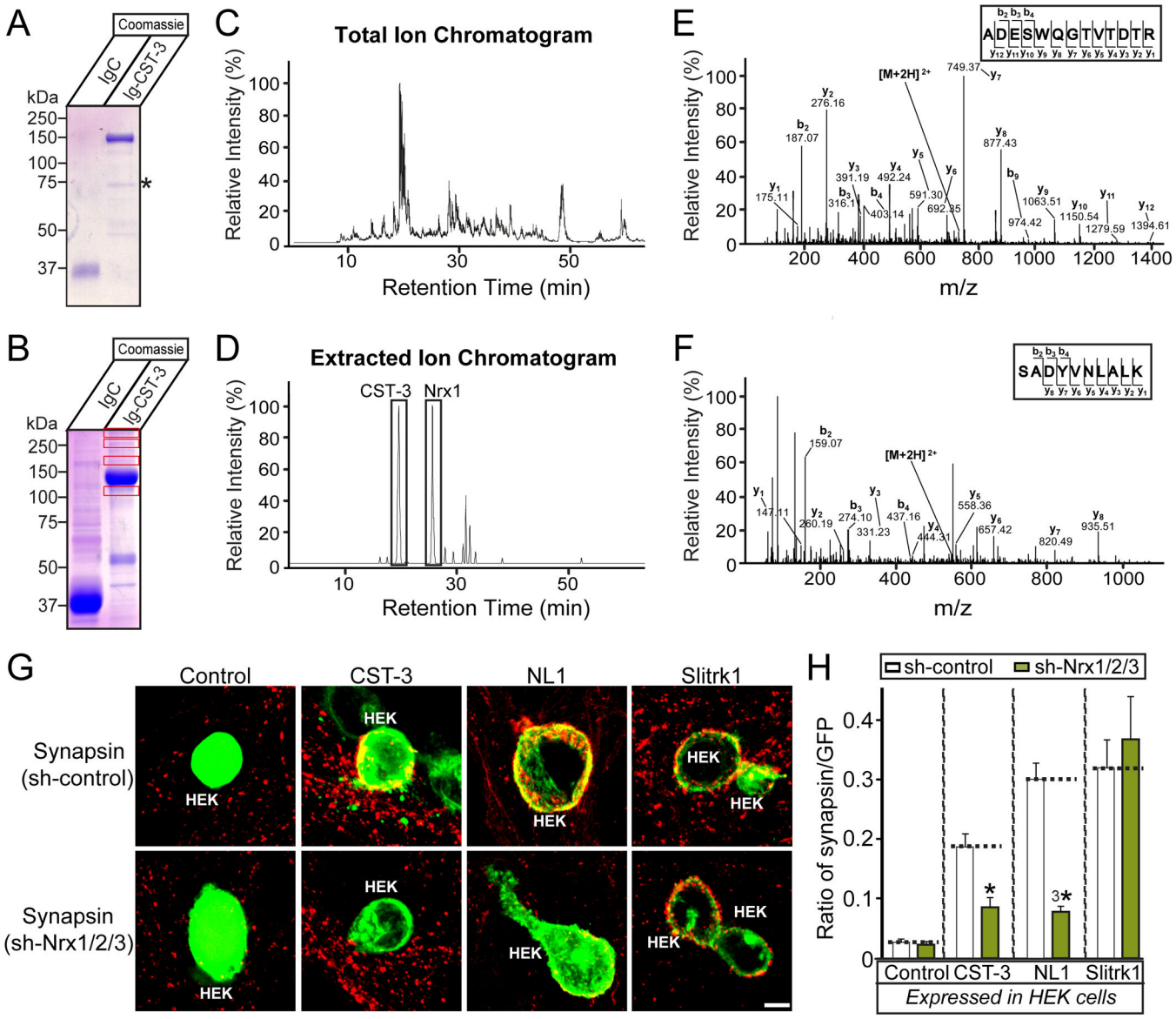

Figure 6. Nrxs Are Functional Receptors For CST-3 To Promote Presynaptic Development

(**A**) Coomassie Blue-stained gel of recombinant Ig-control (IgC), and Ig-CST-3 (Ig-CST-3) fusion proteins used for affinity chromatography and pull-down experiments. (**B**) Identification of specific CST-3-binding proteins in mouse brains. Solubilized mouse brain proteins were subjected to pull-down experiments with IgC or Ig-CST-3-fusion protein. Equivalent amounts of bound proteins were resolved using SDS-PAGE, and the gels were subsequently Coomassie Blue-stained. The boxed regions indicate the specific bands unique to the Ig-CST-3-bound fraction, which were further analyzed through mass spectroscopy. (**C–D**) Mass spectrometry data. Total ion chromatogram (XIC) of an LC separation from Ig-CST3-bound eluates (**C**). Extracted ion chromatogram (EIC) of ion m/z 733.33 and 547.29 from CST-3 (19.30 min) and Nrx-1α (25.77 min; **D**). (**E–F**) The MS/MS spectrum of two double-charged peptides unique for CST-3 and Nrx-1α obtained from LC-MS/MS at 733.33 and 547.29, fragmented to produce an MS/MS spectrum with β- and ψ-ion series describing

the sequences ADESWQGTVTDTR (aa 684–696) and SADYVNLALK (aa 327–336). (**G–H**) The effect of triple Nrx knockdown (sh-Nrx1/2/3) on the synaptogenic activities of CST-3, NL1, and Slitrk1. Representative immunofluorescence images (**G**) of cocultures stained with antibodies to mVenus or HA (green) and synapsin (red). Coincident signals are indicated in yellow. Scale bar = 10 μm (applies to all images). Quantitation (**H**) of heterologous synapse-formation assays, measured as the ratio of synapsin to mVenus/HA fluorescence signals. The dashed lines correspond to the Control values used as the baseline. The data are shown as the means ± SEMs (^{3}*$p<0.001$ and *$p<0.05$ using analysis of variance [ANOVA] with Tukey's test; "n" denotes the total number of HEK293T cells analyzed, as follows: Control/sh-control, n=19; Control/sh-Nrx1/2/3, n=45; CST-3/sh-control, n=43; CST-3/sh-Nrx1/2/3, n=39; NL1/sh-control, n=30; NL1/sh-Nrx1/2/3, n=28; Slitrk1/sh-control, n=24; and Slitrk1/sh-Nrx1/2/3, n=29).

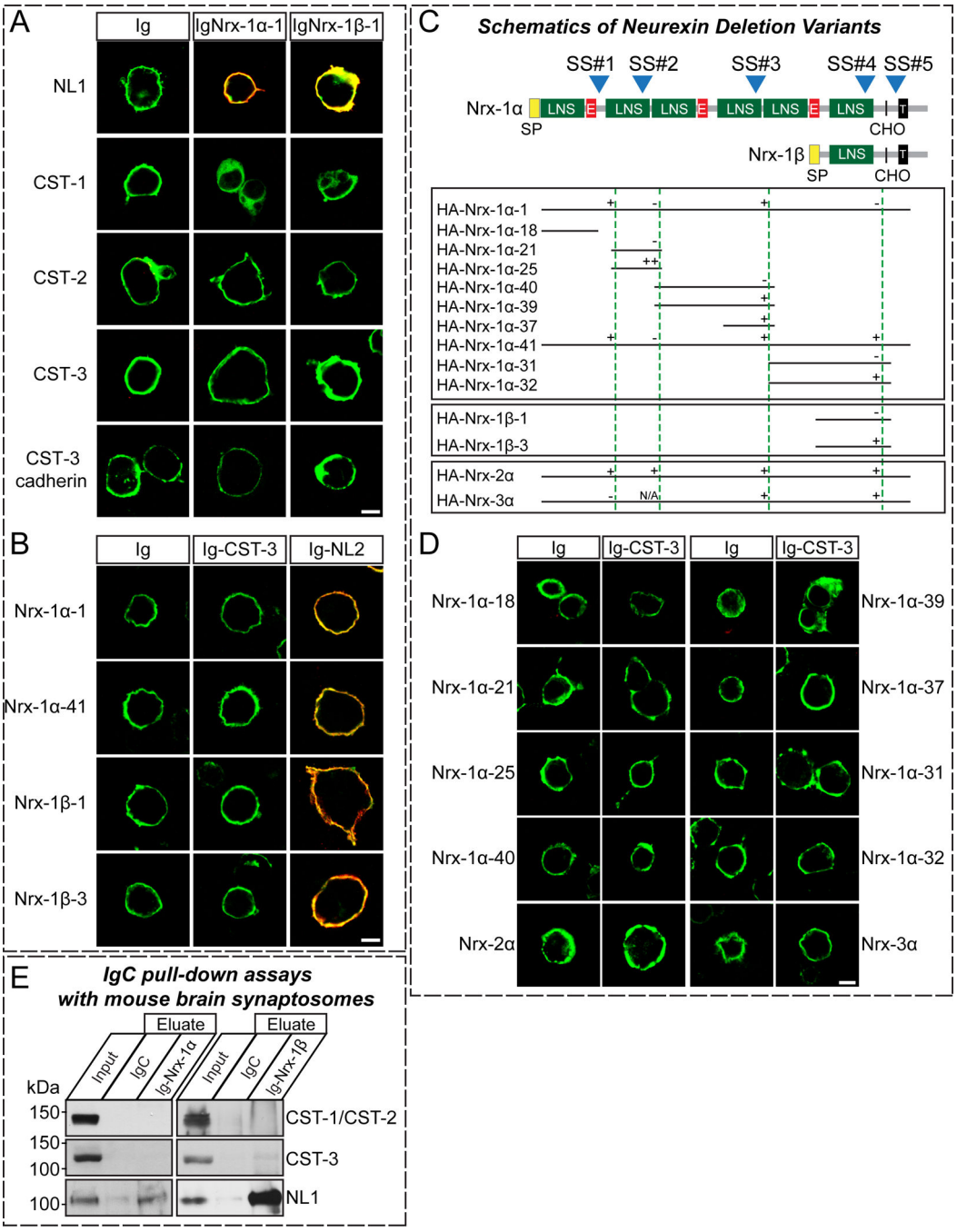

Figure 7. Nrxs Do Not Directly Interact with CST-3

(**A**) Cell surface-labeling assays. HEK293T cells expressing NL1-mVenus (NL1), or HA-tagged CSTs (CST-1, CST-2, CST-3, or CST-3 Cad) were incubated with control Ig-fusion proteins (Ig) or IgNrx-1α-1, or IgNrx-1β-1 (Ig-fusion proteins of neurexin-1α and −1β, respectively, lacking an insert in splice site #4). The cells were analyzed by immunofluorescence imaging for Ig-fusion proteins (red) and HA/mVenus (green). Representative merged images are shown. Scale bar = 10 μm (applies to all images). (**B**) Cell surface-labeling assays. HEK293T cells expressing pcDNA3-FLAG-Nrx vectors were

incubated with Ig, Ig-CST-3 proteins (Ig-CST-3) or Ig-neuroligin-2 (Ig-NL2). The cells were analyzed by immunofluorescence imaging for Ig-fusion proteins (red) and FLAG (green). The only representative merged images are shown. Scale bar = 10 μm (applies to all images). (**C**) Domain structures of α- and β-Nrxs (top) and identities of pDisplay-Nrx constructs used for binding studies (bottom). SP, signal peptide; LNS, Lamin G-domain repeats, neurexins, and sex hormone-binding globulin; E, EGF-like sequences; CHO, carbohydrate attachment site; T, transmembrane region; blue numbered arrows, positions of canonical alternative splice sites (Ullrich et al., 1995). "-" corresponds to the no-insert variant, "+" corresponds to the small insert, and "++" corresponds to the large insert (see (Sugita et al., 2001)). N.A., not applicable. (**D**) Cell surface-labeling assays. HEK293T cells expressing pDis-Nrx-α constructs were incubated with control Ig or Ig-CST-3. The cells were analyzed by immunofluorescence imaging for Ig-fusion proteins (red) and HA (green). Representative merged images are shown. Scale bar = 10 μm (applies to all images). (**E**) Pull-down assays in solubilized mouse synaptosomal fractions. The pull-down assays were performed using IgC (control), IgNrx-1α-1 or IgNrx-1β-1 recombinant proteins. Equivalent amounts of bound proteins were analyzed using the antibodies indicated on the right side of the panels (Input = 5% of total).

Table 1

α-Nrx Proteins as CST-3 Complexes Identified Through LC-MS/MS

Accession No	Gene name	Protein description	Mascot score	Peptide matches
Q9CS84	Nrx-1α	Neurexin-1α	130	59
Q63374	Nrx-2α	Neurexin-2α	26	29
Q6P9K9	Nrx-3α	Neurexin-3α	70	48

Accession numbers refer to the Uniprot/SwissProt database.